

Range and Velocity Measurement with a Bi-static LiDAR System Based on Optical Phased Array

Weihan Xu ⁽¹⁾, Xianyi Cao ⁽¹⁾, Qiqi Yuan ⁽¹⁾, Chuxin Liu ⁽¹⁾, Yuyao Guo ⁽¹⁻²⁾, Liangjun Lu ⁽¹⁻²⁾, Kan Wu ⁽¹⁾, Jianping Chen ⁽¹⁻²⁾, Linjie Zhou ⁽¹⁻²⁾

⁽¹⁾ State Key Laboratory of Advanced Optical Communication Systems and Networks, Shanghai Key Lab of Navigation and Location Services, Shanghai Institute for Advanced Communication and Data Science, Department of Electronic Engineering, Shanghai Jiao Tong University, Shanghai 200240, China

⁽²⁾ SJTU-Pinghu Institute of Intelligent Optoelectronics, Pinghu 314200, China
wei.xu@sjtu.edu.cn

Abstract: Based on a linearly-chirped DFB laser and two multi-layered Si₃N₄-On-Si optical phased arrays, bi-static frequency-modulated-continuous-wave (FMCW) ranging and velocimetry are demonstrated at a ranging resolution of 8 mm and a velocity resolution of 1.6 mm/s. © 2024 The Author(s)

1. Introduction

Solid-state Lidar systems based on photonic integrated circuits (PICs) have received a growing interest for their software-defined scanning patterns and compact form factor [1-3]. One of the promising candidates is the optical phased array beam-steerer based on the silicon-on-insulator platform [4, 5], which boasts digitally addressable yet seamless scanning without external optics. We have previously demonstrated a fully integrated Lidar transmitter [6] based on the multi-layered Si₃N₄-On-Si platform. This chip-scale transmitter comprises a 256-channel optical phased array (OPA) of sparse array geometry and a hybrid-integrated external cavity laser. The device has demonstrated a record-high spatial resolution of 0.051°×0.016° in a state-of-the-art field of view of 140°×30°, while the on-chip laser achieved narrow-linewidth operation at a high output power of 18 mW with a tuning range of approximately 100 nm. Fig. 1(a) depicts the composition of the OPA chip.

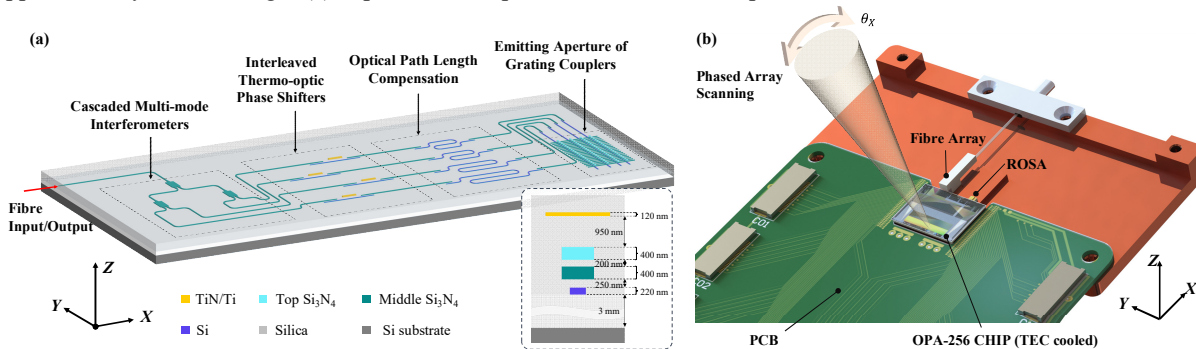


Fig. 1: (a) Schematic of the optical phased array based on the multi-layered Si₃N₄-On-Si platform; (b) A rendering of the packaged solid-state LiDAR TX/RX based on the optical phased array.

Here, we report the experimental results employing the aforementioned chips both as the transmitter (TX) and the receiver (RX). As shown in Fig. 1(b), a one-dimensional scanning in the phased array axis is performed for multi-depth target ranging. With a linearly chirped DFB laser, the solid-state lidar system demonstrated a ranging resolution of 8 mm and a velocity resolution of 1.6 mm/s. The continuous-wave laser power is amplified to 2W before the TX to overcome the link budget limitations due to the limited aperture size and the bi-static mode mismatch. The experiment indicates no penalty on the photonic integrated circuit or the chirped ranging scheme during high-power operation.

2. Experimental Configuration

As prerequisites, both the TX and RX optical phased arrays are calibrated according to our previous work [6] to compensate for the phase error as well as to generate the root look-up-table for beam-steering based on the tilting and sampling of the phase front. Additionally, the pre-distorted driving signal is generated for the DFB laser according to [7] at the operating wavelength of 1549.1 nm with an output power of 10 mW. The symmetric triangle frequency chirp has a bandwidth of 26 GHz at a repetition rate of 1 kHz.

As shown in Fig. 2(a), the pre-distorted driving signal from an arbitrary waveform generator (AWG) is applied to the DFB. The laser output power is first amplified with an erbium-doped fibre amplifier (EDFA) up to 33 dBm and then split into two channels of 1.98 W and 20 mW optical power. The former is launched into the transmitting OPA via the fibre array, while the latter is used as the reference light to provide the coherent gain. The light is launched from TX via the emitting aperture and received by the RX OPA. The signal and reference light beams are combined with a 50/50 fibre coupler and detected by a balanced photodetector (BPD). An oscilloscope (OSC) records the beat signal for spectrum analysis and subsequent range and velocity retrieval. For beam-forming and beam-steering, both OPAs are driven by a deck of digital-to-analogue converters (DACs) for synchronized beam control in the far field. As a proof-of-concept verification, a one-dimensional target of 3 depths is constructed for range-resolution validation ①, while a vibrating steel ruler of high reflectance is used for velocimetry demonstration ②.

3. Results & Discussions

As shown in Fig. 2(b), a LEGO set coated with high reflectance tape is used for ranging resolution validation. The three depths w.r.t. the nearest panel (Depth 2) are approximately 32 mm, 0 mm, and 8 mm. The OPA is scanned at a 0.4° step, starting from the middle of the nearest panel (0°) to both sides, while a SWIR camera is used for bi-static alignment. The range is reconstructed from the peak frequency of the beat spectrum according to

$$R = 0.5c(f_{b,up} + f_{b,down})T_C / 4B \quad (1)$$

where c is the light speed in the free space, $f_{b,up}$ and $f_{b,down}$ are the beat frequencies during the upward and downward chirp durations, T_C is the period of the triangle frequency chirp, and B is the chirp bandwidth. As shown in Fig. 2(c), the one-dimensional scan resembles the target with high fidelity, especially when the depth is reconstructed from the most frequent value (i.e., the numerical mode) of the peak frequency of the beat spectra over 5 periods. Meanwhile, the average (i.e., the numerical mean) and the corresponding standard deviation for each angle are also provided for reference. Based on these results, a ranging resolution of sub-8-mm can be guaranteed with a ranging error within ± 1 cm without interpolating the beat spectrum.

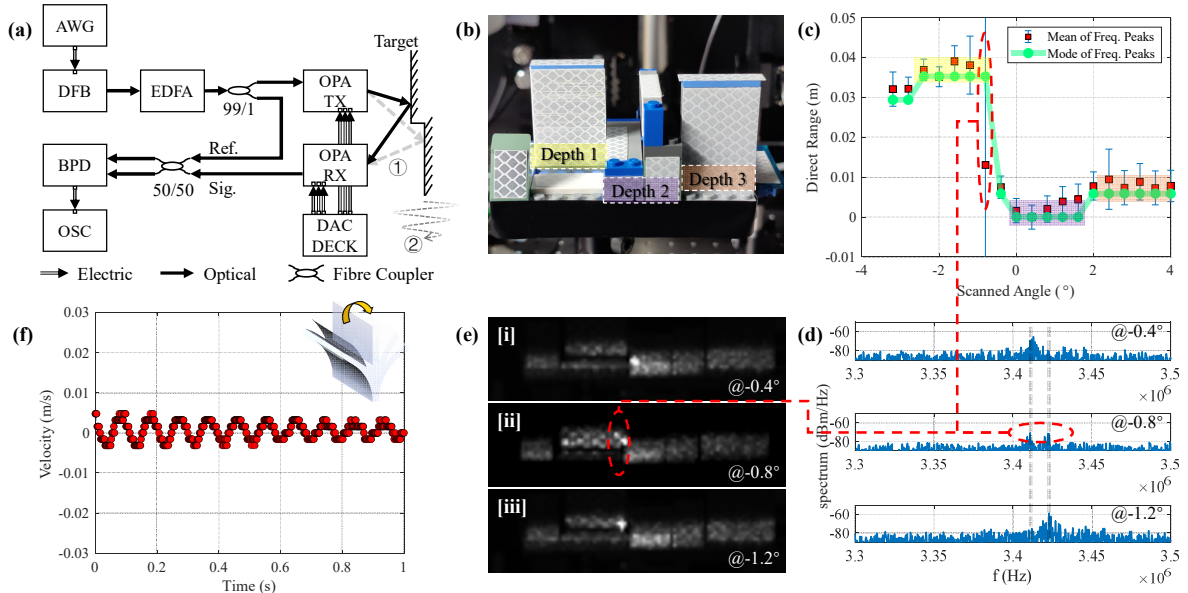


Fig. 2: (a) Experimental setup for the FMCW ranging ① and velocimetry ② with OPAs as solid-state beam scanners in both TX and RX; (b) Picture of the scanned target of 3 depths; (c) Ranges retrieved from the peak frequencies of the beat signal spectra; (d) Spectra of three beat signals from -0.4° to -1.2° ; (e) [i-iii] SWIR images at the three scanning angles; (f) Bi-static velocimetry results of a vibrating steel ruler over one second, inset depicting the vibration of the ruler.

Additionally, based on the bi-static setup, the vibration of a steel ruler is measured based on the Doppler frequency shift between the incident wave and the returned wave. The velocity is reconstructed from

$$v = 0.5(f_{b,down} - f_{b,up})\lambda_0 \quad (2)$$

where the λ_0 is the central wavelength of the chirped laser. As shown in Fig. 2(f), the velocity during the vibration of the ruler exhibits a standard damped oscillation pattern since one end of the ruler is fixed to the optical table. As the

ruler becomes still, the speed gets so slow that the measured speed is no longer resolvable from neighbouring points. The interval between the staircases formed from the unresolvable speed in Fig. 2(f) is 1.58 mm/s.

Finally, among the ranging results, it is worth noting that the 1-D phase scan captures a special incidence at the angle of -0.8° where the TX OPA illuminates both Depth 1 and Depth 2, resulting in a significant disagreement between the mean and the mode of the peak frequency. Fig. 2(d) depicts the beat signal spectra for incidences -0.4° to -1.2° , while the corresponding SWIR images are shown in Figs. 2(e) [i-iii]. At the angle of -0.8° , two peaks coexist while the peak level is further reduced, resulting in the mismatch between the mean and mode of the peak frequencies and the large standard deviation for this specific incidence. Another observation is that the use of sparse OPA with a higher noise level allows for the entire target to be illuminated to some extent by the transmitter. Therefore, based on the spectrum result of -0.8° and the illumination shown in Figs. 2(e) [i-iii], return signals from all depths may coexist in a single spectrum, permitting FLASH-like FMCW ranging capability.

Nevertheless, due to the spatial confinement of the optical table and the strong directivity of bi-static Lidars, only the main lobe would satisfy the phase alignment condition at the RX for our current setup. A quasi-monostatic configuration like Figs. 3(a-b) is being investigated for a smaller mode mismatch between the TX and RX, potentially leading to both a lower link loss and FLASH-like FMCW-ranging results using the background illumination of the sparse array. As shown in Fig. 3(c), preliminary results indicate that at least two depths are presented in the single spectrum, while Depth 3 may be aliased with Depth 2 due to the higher noise floor. We are working on further link loss reduction to demonstrate both FLASH-like ranging and direction of arrival (DOA) reconstruction based on our sparse OPAs.

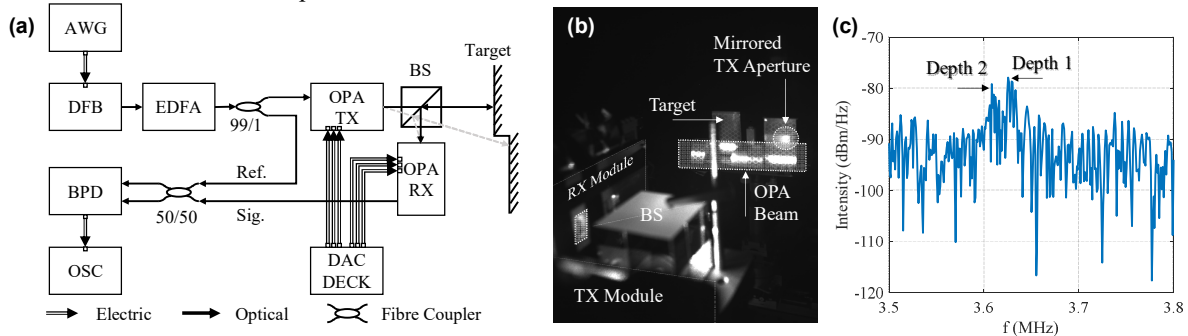


Fig. 3: (a-b) The schematic and SWIR picture of the quasi-monostatic LiDAR setup under investigation; (c) The preliminary beat-signal spectrum of FLASH-like ranging of multiple targets.

4. Conclusions

We demonstrated a bi-static lidar incorporating a linearly-chirped DFB laser and two Si_3N_4 -On-Si optical phased arrays for 1-D phased array ranging and radial velocimetry. Compared to our previous work with fibre collimators, the setup operates at an input power level of nearly 2W through a pair of transceiving OPAs without observable penalty. The range and speed resolution are 8 mm and 1.58 mm/s, respectively. Long-range operation or FLASH-like FMCW ranging of multiple targets can be extrapolated with a lower link loss.

Reference

1. N. Li, C. P. Ho, J. Xue, L. W. Lim, G. Chen, Y. H. Fu, and L. Y. T. Lee, "A Progress Review on Solid-State LiDAR and Nanophotonics-Based LiDAR Sensors," *Laser & Photonics Reviews* **16**, 2100511 (2022).
2. M. R. Watts, C. Poulton, M. Byrd, and G. Smolka, "Lidar on a Chip Enters the Fast Lane: Sensors for Self-Driving Cars and Robots will be Tiny, Reliable, and Affordable," *IEEE Spectrum* **60**, 38-43 (2023).
3. S. Lin, Y. Chen, and Z. J. Wong, "High-Performance Optical Beam Steering With Nanophotonics," *Nanophotonics* **11**, 2617-2638 (2022).
4. K. Van Acoleyen, W. Bogaerts, J. Jágerská, N. Le Thomas, R. Houdré, and R. Baets, "Off-Chip Beam Steering With a One-Dimensional Optical Phased Array on Silicon-on-Insulator," *Optics letters* **34**, 1477-1479 (2009).
5. J. Sun, E. Timurdogan, A. Yaacobi, E. S. Hosseini, and M. R. Watts, "Large-Scale Nanophotonic Phased Array," *Nature* **493**, 195-199 (2013).
6. W. Xu, Y. Guo, X. Li, C. Liu, L. Lu, J. Chen, and L. Zhou, "Fully Integrated Solid-State LiDAR Transmitter on a Multi-Layer Silicon-Nitride-on-Silicon Photonic Platform," *Journal of Lightwave Technology* **41**, 832-840 (2023).
7. X. Cao, K. Wu, C. Li, G. Zhang, and J. Chen, "Highly Efficient Iteration Algorithm for a Linear Frequency-Sweep Distributed Feedback Laser in Frequency-Modulated Continuous Wave Lidar Applications," *J. Opt. Soc. Am. B* **38**, D8-D14 (2021).